Optical and photoelectric properties of alkali metals

J. Monin and G.-A. Boutry

Conservatoire National des Arts et Métiers Paris 3ème, and Laboratoires d'Electronique et de Physique appliquée, Limeil-Brévannes, France 94450

(Received 5 July 1973)

The paper gives, in the form of tables and graphs, the optical constants and photoelectric emisssion for the four alkali metals Cs, Rb, K, and Na in the spectral range 250–630 nm inside which the volume-plasmon wavelengths λ_p and the surface-plasmon wavelength λ_s are situated. The metals are prepared in the form of optically thick layers condensed in ultrahigh vacuum (10^{-11} torr) on targets cooled at 77 °K. When maintained at 77 °K, the layers show a spectral selectivity independent of the state of polarization of the exciting monochromatic radiation. Upon reheating at 195 °K or higher, a very pronounced vectorial selectivity appears, accompanied by diminution of the photoemission. Values given in the tables and graphs are reproducible within a fair approximation, stated in each case. From the "optical" conductivity curves $\sigma = f(\hbar\omega)$, it is not possible to identify an absorption process due to interband transitions (Wilson-Butcher theory). The plot of the real part of the dielectric constant against the square of the exciting radiation wavelength $\epsilon_1 = f(\lambda^2)$ is perfectly linear for all reheated layers, thus allowing use of the Cohen and the Fowler formulas in the calculation of σ, λ_p, the "optical" mass, the polarizability, and the work function for several temperatures. The normal reflectivity curves for the reheated layers show a point of inflection for $\lambda = \lambda_P$. For the same layers, the quantum efficiency of the photoemission shows a minimum for $\lambda = \lambda_p$, particularly well marked for the lighter metals. Finally, the work-function values at 0 °K extrapolated from our experimental results by the Fowler process, are shown to have two values $W_{||}$ and $W_{\perp}$ whenever the layer investigated exhibits vectorial selectivity; the difference $W_{||} - W_{\perp}$ is only a few hundredths of an electron volt but is quite reproducible.

I. INTRODUCTION

The principal purpose of this paper is to provide reliable and reproducible data on which future theories of photoemission in alkali metals may be securely based. The major publications on the subject are listed and discussed briefly in the recent papers of Smith and Spicer,[1] who have performed an investigation somewhat similar to ours, on sodium and potassium. However, there are several points of disagreement between their results and the data contained in the present paper. Our results deviate also very considerably from those of Mayer and Thomas.[2] Since all these papers relate to work done under fair ultrahigh vacuum conditions, we describe here briefly, but carefully, our experimental setup and procedures, in order that other experimenters may experience no difficulty in checking our results. With the classical work of Ives and co-workers,[3] there are also points of disagreement, more easily explained by the fact that the pioneer work of Ives was performed during the 1930's, a period when it was practically impossible to operate under pressures much lower than 10^{-7} torr.

We have not experimented on lithium. Regarding sodium, we should draw the attention of the reader to the fact that the exact crystalline structures of the layers on which we made our measurements was not known with certainty: both sodium and lithium seem to have several possible crystalline structures at room temperature or lower,[4] so that the solid phase may be a mixture of these structures in unknown proportions (the specific gravity usually attributed to sodium is also abnormal, being larger than that for potassium, respectively 0.97 and 0.86): we shall see that the crystalline structure may be one of the major parameters governing optical and photoelectrical properties. However, our results for Na agree fairly well with those of Van Oirschot,[5] who has worked under the same indetermination.

II. EXPERIMENTAL

A. Material

"Chemically pure" (impurity content always smaller than 0.05%) metals were purchased in sealed Pyrex tubes from several reliable firms (Chemische Fabrik, Görlitz; Kawecki Beryl Co., U.S.A.). Each sample was treated by fractional distillation *in vacuo* (about 10^{-8} torr), a process that lasted for about 10 h: it was necessary to avoid chemical action of the alkali vapor on the inside surface of the distillation chamber, so that the temperature had to be kept low ($\theta \leq 140$ °C for Cs; $\theta \leq 155$ °C for Rb; $\theta \leq 180$ °C for K). The outgassed and purified final product was then distributed between a number of Pyrex bulbs each containing about 0.2 G of metal. These were sealed and stored till needed. The design of the bulbs made them easy to break under vacuum with a Pyrex-coated outgassed magnetic hammer.

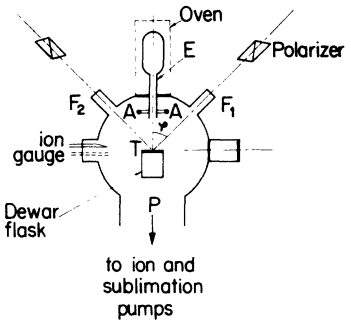

FIG. 1. Schematic of the vacuum chamber.

B. Vacuum chamber

The metal layers were prepared and their properties measured in a stainless-steel vacuum chamber built for this purpose. Figure 1 is a schematic drawing of the setup of the chamber itself. The metal layer to be investigated is deposited on the target T, a disk of optically plane borosilicate glass with a metal-rim contact. This target is part of the wall of a metallic Dewar flask which may be filled with various cooling mixtures to fix the temperature of the target surface. With the help of a Tombac mounting and of three screws, the orientation of the target may be modified at will.

The metal vapor issues from the evaporation funnel E, which has been designed and collimated in such a way that the amount of metal not deposited on the target is negligible. The evaporator funnel may be opened or closed by a movable shutter (not shown in Fig. 1). Between evaporator and target, out of range of the metal vapor, the electrically insulated ring A acts, when desirable, as the anode collecting the photoelectrons issuing from the layer surface when illuminated. All necessary temperature measurements were made with suitably located thermocouples.

Plane-polarized monochromatic light issuing from the exit slit of a quartz-prism monochromator (supplemented with interference filters to expel any diffuse radiation of unwanted wavelength) enters the cell by a fused-quartz window F_1 and falls on the target at incidence 45°. The reflected light leaves the cell through a similar window F_2; the divergence of the beam is negligible. The light issuing from F_2 proceeds through to an ellipsometer (which will be considered later). The photoelectric emission is computed from the measurement with a calibrated photomultiplier of the light incident on F_1 and of the saturated photocurrent given by the photocathode T to the collecting anode A.

The vacuum chamber is evacuated through the rear opening P by a conventional ultrahigh-vacuum pumping system featuring a cryoadsorption roughing pump, an ionization-adsorption pump, and a titanium sublimator. Outgassing and pumping this complete unit (over-all baking temperature about 300 °C) takes 24 h; the residual pressure is estimated by extrapolation from the indications of a Bayard-Alpert ionization gauge. During metal deposition, this pressure was about 5×10^{-11} torr; during measurements, the actual pressure decreased a little (between 2×10^{-11} and 3×10^{-11} torr).

The complete unit, cell plus pumping system, is mounted on a movable base which may be clamped in a precisely reproducible position on the ellipsometric bench.

C. Deposition procedure

In all cases, we start from one of the sealed bulbs described in Sec. IIA. The sealing technique, through the short-duration overheating necessary to melt the glass, always releases minute quantities of gas, some of which were trapped inside the bulb. By way of consequence, breaking the bulb in ultrahigh vacuum is always accompanied by a small rise in the residual pressure which subsides after a few seconds. To avoid possible contamination of the future layer, the metal is first distilled twice under a residual pressure of $\sim 10^{-10}$ torr, then transferred into the evaporator itself; finally, the evaporator is heated, the shutter is opened, and deposition proceeds on the target which, during the whole proceedings, is kept at a temperature of 77 °K. The evaporator unit is heated under control of a thermocouple. Provided that the target has been well cleaned and outgassed and that the evaporation rate is chosen correctly, a mirrorlike surface layer develops, the optical properties and photoemission being followed and measured during deposition. For instance, in the case of rubidium, an evaporation time of 75–90 min is indicated and will produce a layer whose optical properties and photoemission remain constant during the last 15–20 min of evaporation, indicating that the layer deposited is thick enough to behave as the bulk metal. It is not always realized that this necessary thickness varies rapidly, in the case of the alkali metals, both with wavelength and incidence φ. From our results we have computed for potassium the thickness d, which will reduce the transmitted flux to 1% of its incidence value (see Table I).

Though the process of evaporation is not as precisely controlled as the other parameters (one recalls that the rate of deposition varies exponentially with temperature), the optical properties of the layers obtained have shown themselves to be quite accurately reproducible, within conditions that will be given later. Large deviations from the operating procedure which has just been described

TABLE I. Thickness of a potassium layer corresponding to an optical density 2.

λ (Å)	d (Å) $\varphi = 0$	$\varphi = 45°$
6200	1300	1200
2536	20000	4500

may result in "shiny" and even diffusing opalescent layers whose optical properties could, of course, not be determined.

Throughout this work, layer deposition was always made on a target cooled to 77 °K. After completion of the deposition, a first set of optical and photoelectric measurements was made, the target and its layer remaining at 77 °K (set 1). These being completed, the target temperature was slowly raised to 195 °K (293 °K in the case of sodium), when a second set of measurements was made (set 2), which gave the universal result of an important variation in the optical and photoelectrical properties of the surfaces. This change was *definite* and *irreversible*. Heating the Na, K, and Rb targets to room temperature caused only negligible shifts in the optical properties; cooling the same targets back to 77 °K did *not* restore the values found in Set 1. Upon heating again, only a very small departure from the results of set 2 could be found. Cesium layers, because of the non-negligible volatility of Cs at ~300 °K, could not be heated to room temperature.

An obvious interpretation of these facts is as follows: At 77 °K the alkali atoms falling on the target have little or no mobility and remain, more or less, where they fall. The layer at 77 °K is thus made up of microcrystals with random orientation and a statistic distribution of size, with a mean grain diameter which remains small compared with the wavelength of the incident monochromatic light. Upon heating the layer, the microcrystallites merge into a macrocrystalline structure with a preferred orientation affecting the quasi total exposed area of the layer. Actually there is some experimental evidence that this is so in the case of potassium: Richard (Laboratoires d'Electronique et de Physique appliquée) and co-workers,[6] using slow-electron diffraction, have shown that layers of potassium deposited on cooled targets of NaCl, KF, and *optically plane borosilicate glass* rearranged themselves, upon heating to 195 °K, into a macrocrystalline structure in which the entire surface of the layer seemed oriented parallel to the (110) plane. We shall see later that some of our results provide experimental evidence in favor of this interpretation.

If this interpretation is correct, one should expect that the reproducibility of the surface properties at 195 °K from experiment to experiment should be much better and much more stable than the surface properties measured at 77 °K immediately after deposition. This is actually the case and, because of that, Secs. III and IV are devoted to an examination of optical and photoelectrical properties of the layers stabilized at 195 and 293 °K. Section V will be devoted to a systematic comparison of the preceding results with those of measurements at 77 °K immediately after deposition. In all cases, the tables indicate the order of magnitude of the possible deviations from one layer to another.

D. Ellipsometer

This instrument has been specially designed and built to do the work described here. We make use of a Faraday rotator technique akin to that used for linearly polarized light.[7] The principles of its operation will be understood easily with the help of Fig. 2: the narrow beam of light issuing from a suitably collimated monochromatic source S is linearly polarized by a Glan prism P, after which the direction of vibration of the electric vector makes an angle θ with the plane of incidence. The polarized beam falls on the surface M under study at a fixed incidence, e.g., 45°. If θ is neither 0° nor 90°, the light regularly reflected by M will be elliptically polarized. The reflected beam enters into a "Faraday rotator," a cylindrical container filled with water and placed in a uniform axial magnetic induction varying sinusoidally with times at a fixed low frequency F (currently 50–135 Hz). The magneto-optic effect induces a sinusoidal variation of the angle γ between the plane of incidence and the axis of the oscillating ellipse.

Issuing from the rotator, the polarized beam goes through a Glan analyzer, followed by the photomultiplier, PM. If the angle (β) between the principal section of the analyzer and the plane of incidence is either γ or $90° - \gamma$, the Fourier spectrum of the electric signal issuing from the PM

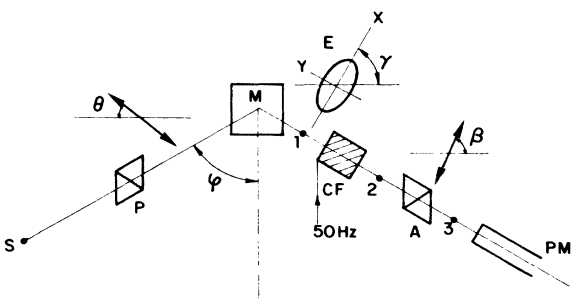

FIG. 2. Ellipsometer principle.

anode will have $2F$ as its lowest frequency. In all other cases, the frequency F will appear in this spectrum. The principle of operation is therefore to find the angle γ for which F disappears from the signal. This can be done with very good sensitivity by passing the PM output through a low-pass filter designed to reject the (always large) $2F$ component, tuning a narrow-bandwidth (0.02 Hz) amplifier on the frequency F, and using synchronous demodulation. With our present apparatus, a rotation of ± 3 sec of an arc is detectable; however, precision and accuracy are limited by imperfections of the polarizer and analyzer circles to a little better than ± 10 sec of an arc. In the best possible case, this corresponds to an uncertainty of 1 part in 10 000 on reflectivity. The wavelength range of measurements was approximately 6300–2400 Å. Needless to say, the quartz windows F_1 and F_2 must be quite free from birefringence.

There are at least two different methods of measurement that may be used with this instrument, a detailed exposition of which has been given elsewhere[8]; one appears better adapted to the measurements on highly reflecting surfaces. However, as the reflecting power increases, the precision on the optical constants decreases. One of us (J. M.) has made a detailed study of the variations of precision in measurement[9]; the results appear in all our optical-constants tables as a column giving the uncertainty of determination.

All ellipsometers, ours included, define the orientation in space of several planes, and therefore what they "measure" are angles. From these angles, the optical constants proper (reflectivities R, real and imaginary parts of the refraction index n and k, "optical conductivity" σ, and the real part of the dielectric constant ϵ_1) are deduced under the assumption that the Fresnel-Maxwell formulas for reflection and refraction in absorbing media are valid in this frequency range and for such metallic targets. It is useful to recall that a consequence of these formulas is that, for the angle of incidence 45°, they *always* give

$$R_{\parallel} = R_{\perp}^2 \quad ,$$

where $R_{\parallel}$ and $R_{\perp}$ are, respectively, the reflectivities of any surface for an electric vector in the plane of incidence and an electric vector perpendicular to this plane.

III. OPTICAL PROPERTIES OF THE BULK METALS ("THICK LAYERS"): 195 and 293 °K

A. Real part of the dielectric constant: "Optical" mass

The energy range of the photons with which we have experimented extends from 2 to 5 eV and falls in the domain of interband transitions in alkali metals. Under such conditions, the real part

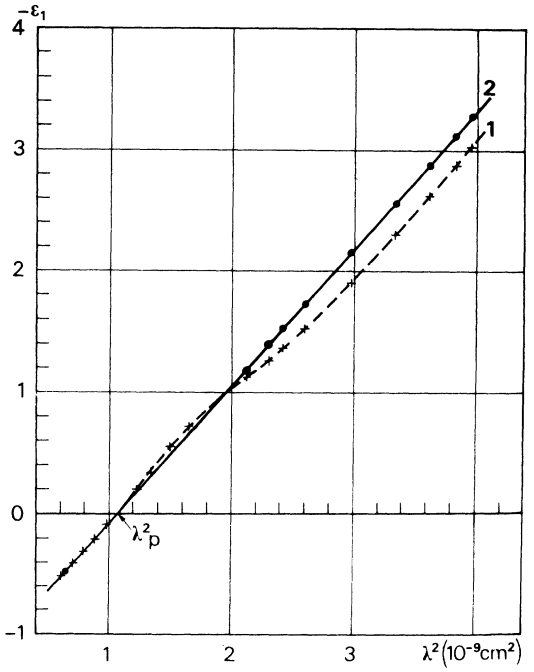

FIG. 3. ϵ_1 vs λ^2 for potassium: 77 °K (1), 195 °K (2).

of the dielectric constant ϵ_1 may be written, according to Cohen[10],

$$\epsilon_1 = 1 + 4\pi N_0 \alpha_1 - \frac{Ne^2}{\pi m_0 c^2}\lambda^2 \quad , \qquad (1)$$

where N_0 is the atomic concentration, N is the conduction-electron concentration, α_1 is a constant polarizability coefficient, and m_0 is the "optical mass." If this relation applies, it is possible to compute from it the polarizability coefficient α_1, the plasma wavelength λ_P [defined as the value of λ for which ϵ_1 vanishes in Eq. (1)] and the "optical mass" m_0 for each metal under study. The graphical representation of Eq. (1) is, in this case, a straight line with a negative slope.

According to our measurements, this is never the case for layers prepared, kept, and measured at 77 °K without any heating, (see Figs. 3 and 4). The same layers studied after heating to 195 °K (293 °K for sodium) show linearity in Eq. (1) to a very high degree of precision (5 parts in 1000 in practically all cases) in the entire range of λ investigated, with the exception of a slight but perfectly reproducible departure from linearity for cesium at wavelength $\lambda = 3340$ Å; this behavior is linked, as we shall see, with an abnormal optical conductivity in the same domain.

The accompanying tables (II–V) give the values of the optical mass, the polarizability and the volume-plasmon wavelength computed from our measurements; we also show the values given by other experimenters in each case.

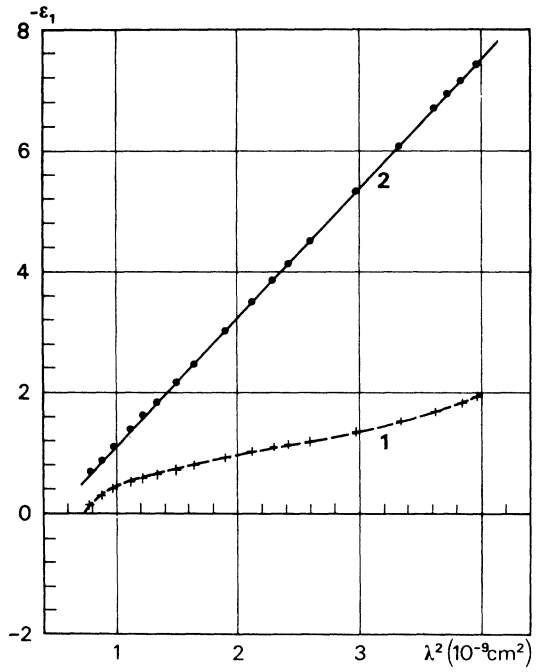

FIG. 4. ϵ_1 vs λ^2 for sodium: 77 °K (1), 293 °K (2).

B. Optical conductivity (or absorption coefficient) $\sigma = \epsilon_2 \epsilon_0 \omega$

Figure 5 sums up our results for σ, as computed for the four metals from our ellipsometric data. The temperature was 195 °K except for sodium, for which the measurements took place at 293 °K. We show on each curve the position of the volume-plasmon wavelength, λ_P. The metals K and Rb show a well-defined maximum for a wavelength λ_m' not too far removed from the surface-plasmon wavelength λ_s; the energy corresponding to λ_m^1 falls in the 2–3-eV range. The curve for cesium exhibits no true maximum located in the range of our measurements, but an anomaly occurs near $\lambda = 5400$ Å which, though small, does not seem due to errors in measurement.

The behavior of sodium is at the same time similar and widely different. For this metal, a quite sharp maximum of σ occurs at 2.58 eV (4860 Å) while the surface-plasmon energy is about 4 eV. Moreover, for the three metals K, Rb, and Cs, σ increases with the atomic number, in contradistinction to the electrical conductivity; sodium is not found in its proper place in this series. We have already mentioned similar anomalies for other physical properties of sodium.

In the range of photon energies $\hbar\omega > \hbar\omega_P$, σ, for the triad Cs, Rb, and K, increases steadily with $\hbar\omega$ towards a possible maximum located in the uv spectrum too far from our range of measurement, except for cesium, for which a possible maximum is located at $\hbar\omega = 5$ eV (about 2500 Å). Arakawa,[11] Smith,[12] and Mayer and Hietel[13] have also measured the σ of cesium, working sometimes with a quartz-metal interface. From Fig. 6, the reader will deduce that their results are in fair agreement with ours. Arakawa has attempted to explain this uv absorption in terms of interband transitions from the conduction band to d and f bands, or, possibly, of the excitation of volume plasmons in this region.

The now classical theory of the "quasifree electrons" postulates that the over-all absorption coefficient σ is the sum of two terms,

$$\sigma = \sigma_D + \sigma_i \quad .$$

The Drude term σ_D represents the absorption induced in the metal by intraband transitions and has the value

$$\sigma_D = \frac{Ne^2}{m^*\omega^2\tau} \quad ,$$

where N is the concentration of conduction electrons, m^* is the effective electron mass in the lattice structure, and τ is the electron relaxation time (τ may be computed from the electrical conductivity of the metal at the relevant temperature).

The interband term σ_i has been computed by Wilson[14] and Butcher[15] and, according to these authors, is given by the expression

$$\sigma_i = \frac{me^2 |V_{110}|^2 (\hbar\omega - \hbar\omega_1)(\hbar\omega_2 - \hbar\omega)}{\pi\hbar^3 G_{110}(\hbar\omega)^3} \quad ,$$

in which G_{110} is a reciprocal-lattice vector and

TABLE II. Optical mass, polarizability, and volume-plasmon wavelength of cesium.

Authors	T (°K)	m_0/m	$4\pi N_0\alpha_1$	λ_P (Å)
Ives and Briggs, (analyzed by Cohen, Ref. 10)	293	1.02 ± 0.02	0.37 ± 0.03	4260
Mayer and Hietel, Ref. 13	293	1.45 ± 0.02	0.17 ± 0.10	4330
C. Kuntz, Ref. 24	293	...	...	4270
N.V. Smith, Ref. 12	293	1.19	...	4130
present paper	195	1.13 ± 0.01	0.32 ± 0.01	4360 ± 10

TABLE III. Optical mass, polarizability and volume-plasmon wavelength of rubidium.

Authors	T (°K)	m_0/m	$4\pi N_0\alpha_1$	λ_p (Å)
Ives and Briggs (Cohen's analysis, Ref. 10)	293	1.08 ± 0.03	0.50 ± 0.05	4120
Mayer and Hietel, Ref. 13	293	1.26	$0.04+0.10$	4000
C. Kunz, Ref. 24	293	...	...	3640
N. V. Smith, Ref. 12	293	1.16	...	3640
Whang *et al.*, Ref. 25	293	1.03 ± 0.02	0.25 ± 0.02	3720 ± 30
present paper	195	1.06 ± 0.01	0.25 ± 0.01	3670 ± 10

V_{110} in the corresponding Fourier component of the pseudopotential. We can get at the value of V_{110} in two ways: (a) by computation from band theory and (b) experimentally from measurements of the de Haas–van Alphen effect. In both cases, the results appear widely divergent from author to author. In the following comparison of our results with the Wilson-Butcher theory, we have used the values of V_{110} given by Ashcroft, [16] who has determined them for the four metals Na, K, Rb, Cs from measurement of the de Haas–van Alphen effect.

Figures 6–9 show the results of this comparison for Cs, Rb, K, and Na and plot at the same time the results of similar measurements of $\sigma=f(\hbar\omega)$ by Arakawa, Smith, Mayer and Thomas, and other authors. It is clear that our results will not fit within the Wilson-Butcher theory. It is also true, unfortunately, that the measured values of σ differ widely between the experimenters, cesium being an exception. It is possible that these vast discrepancies arise from the high reflectivity of the three metals Na, K, and Rb in the spectral range concerned. The determination of σ from ellipsometer measurements becomes inaccurate in such a case: For instance, in the case of potassium at 6200 Å, to get $\Delta\sigma/\sigma\simeq 10\%$, the ellipsometric angular determination must be made with an accuracy better than 1 min of an arc (at incidence 45°).

We should pay particular attention to the results of Smith, who has used the ellipsometric method to study the four metals in the range 0.5–4 eV, with an ellipsometer specially built for the purpose. Taking into account a mean probable error of ± 5%, Smith's values are in fair agreement with ours for sodium only; for potassium and rubidium, his results and ours diverge increasingly with increasing wavelength ($\lambda>5000$ Å for K; $\lambda<5500$ Å for Rb).

Our determinations show an absorption maximum between 2 and 3 eV, which we might attribute to a surface effect of some sort. Excitation of surface-plasmon or electrical-polar resonances associated with surfaces defects; photoemission results (see Sec. IV) seem to agree with this interpretation. In such cases, the surface would appear nonhomogenous, behaving like a skin clothing the bulk crystal and the validity of the classical computation of σ from the Maxwell-Fresnel theory of metallic reflection with an infinitely-thin-metal–vacuum interface would become doubtful.

C. Reflectivity

The reflectivity R_0 for normal incidence has been computed from ellipsometer measurement through the calculation of the optical constants n and k with the help of the formula

$$R_0=\frac{(n-1)^2+k^2}{(n+1)^2+k^2}\ .$$

TABLE IV. Optical mass, polarizability, and volume-plasmon wavelength of potassium.

Authors	T(°K)	m_0/m	$4\pi N_0\alpha_1$	λ_p (Å)
Ives and Briggs (Cohen's analysis, Ref. 10)	293	1.80 ± 0.02	0.28 ± 0.05	3380
Mayer and Hietel, Ref. 13	293	1.00	0.11 ± 0.10	2920
C. Kunz, Ref. 24	293	...	...	3330
J. Brambring, Ref. 26	78	...	...	3270 ± 10
Sutherland and Arakawa, Ref. 27	293	1.06 ± 0.03	0.20 ± 0.03	3330 ± 50
N. V. Smith, Ref. 17	293	1.06	0.20	3260 ± 80
Palmer and Schnatterly, Ref. 28	293	0.98	0.25 ± 0.05	3220
present paper	293	1.06 ± 0.01	0.20 ± 0.01	3280 ± 10
	195	1.08 ± 0.01	0.20 ± 0.01	3270 ± 10

TABLE V. Optical mass, polarizability, and volume-plasmon wavelength of sodium.

Authors	T(°K)	m_0/m	$4\pi N_0\alpha_1$	λ_p (Å)
Ives and Briggs (Cohen's analysis, Ref. 10)	293	1.01 ± 0.02	0.10 ± 0.08	2200
Mayer and Hietel, Ref. 13	293	1.17 ± 0.03	0.15 ± 0.10	2260
C. Kunz, Ref. 24	293	•••	•••	2170
Sutherland and Arakawa, Ref. 27	293	1.16 ± 0.05	0.03 ± 0.02	2180 ± 20
N. V. Smith, Ref. 17	293	1.07	•••	2200 ± 40
Palmer and Schnatterly, Ref. 28	293	0.96	0.34	2360
present paper	293	1.07 ± 0.01	0.04 ± 0.02	2210 ± 10

Figure 10 shows the variation of R_0 with wavelength for thick layers of the four metals, after "heating" at 195 °K (293 °K for sodium). All curves are of the "silver type," dropping rapidly in the near ultraviolet to values which become very small at 2650 Å, $R_0=0.011$ for cesium, 0.018 for Rb, 0.048 for K: the smaller the atomic number of the element, the steeper the slope. Our equipment did not permit experimenting farther in the uv than 2300–2400 Å, and hence observing the dropping of R_0 to its minimum in the case of sodium.

The slopes of these $R_0=f(\lambda)$ curves are actually never as small at the red end of the spectrum as is the case for silver; alternately, the slopes in the uv are not as large. Attention should be paid to the fact that the second derivative $d^2\lambda_0/d\lambda$ changes its sign for wavelength λ_p, the value of the volume-plasma wavelength as computed from the Cohen formula for $\epsilon_1=0$ (see Tables II–V).

For any wavelength, the reflectivity of the four metals increase with decreasing atomic number. The greatest reflectivity computed from our measurements is for sodium at 6200 Å: its value, $R_0=98.2\pm0.3$, is very large indeed.

We sum up our results regarding optical properties of the four metals in the 2500–6300-Å range in Tables VI–IX. Values of ϵ_1, σ, R_0, n, and k are listed together with the maximum error of lack of reproductibility in each case. These tables should be compared with those given by Smith for sodium and potassium[17] and for rubidium and cesium.[12]

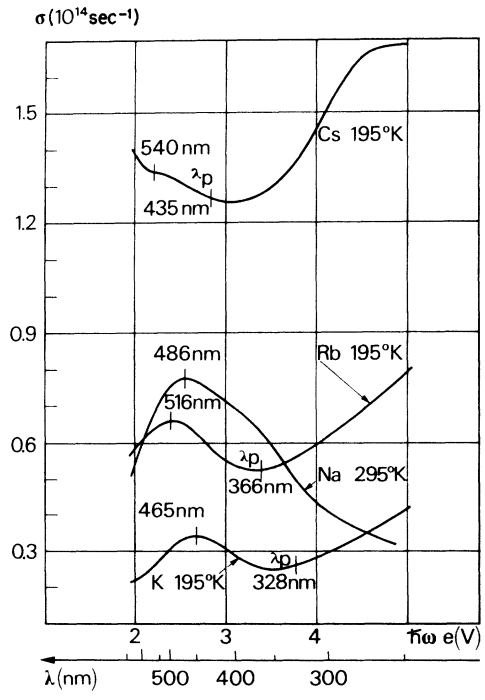

FIG. 5. Optical conductivity of Cs, Rb, K, and Na.

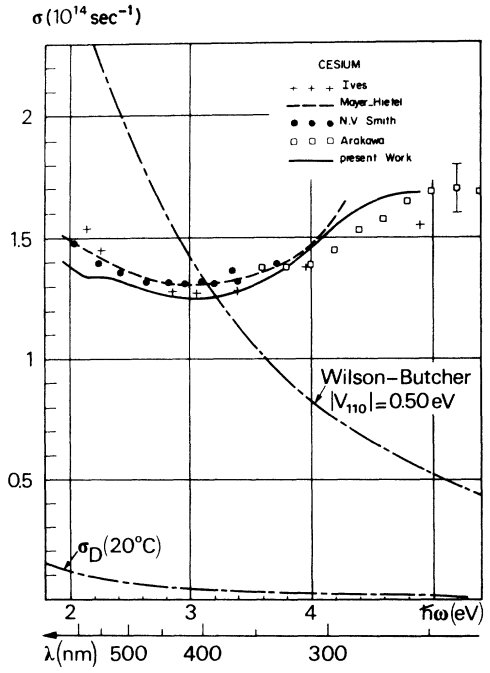

FIG. 6. Optical conductivity of cesium: results of this paper, of previous workers, and of theory.

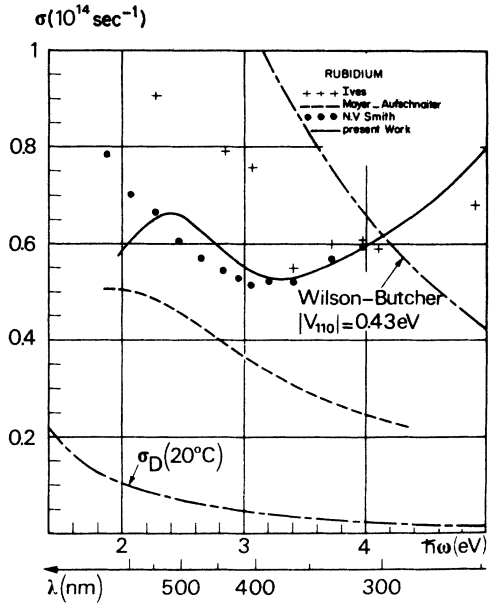

FIG. 7. Optical conductivity of rubidium: results of this paper, of previous workers, and of theory.

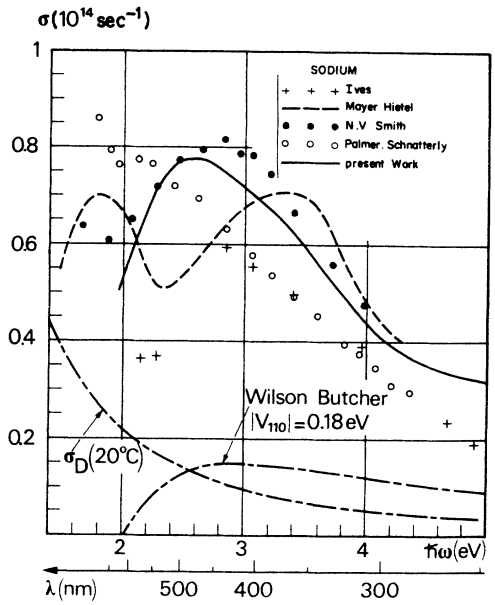

FIG. 9. Optical conductivity of sodium: results of this paper, of previous workers and of theory.

IV. PHOTOEMISSION OF THE BULK METALS (THICK LAYERS, 195 AND 293 °K)

Call the photocurrent i, the incident power flux w_i, and the reflectivity R for an incidence angle $\varphi = 45°$. The *emissivity* S_λ and the "true" quantum efficiency are defined by

$$S_\lambda = \frac{i}{w_i} = f(\lambda); \quad Q_\lambda = \frac{S_\lambda}{1-R}\,\frac{\hbar\omega}{e} \quad .$$

S_λ and Q_λ have both been measured using plane polarized monochromatic beams of light, the electric vector being in the plane of incidence of the light ($E_\parallel$) in one set of measurements and perpendicular to this plane ($E_\perp$) for the other.

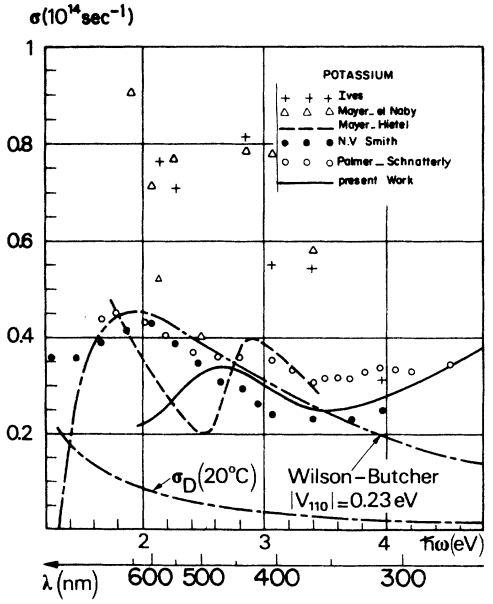

FIG. 8. Optical conductivity of potassium: results of this paper, of previous workers and of theory.

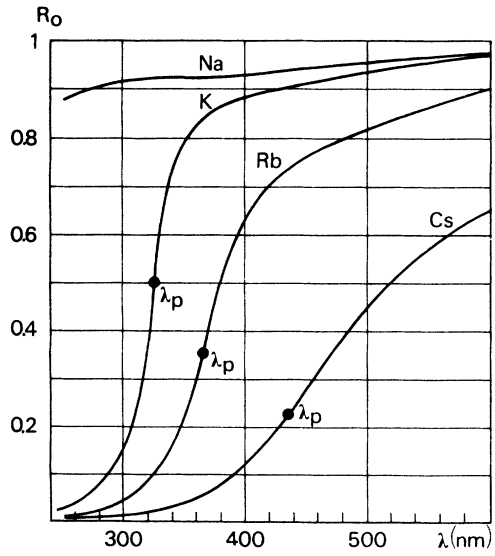

FIG. 10. Reflectivity of Cs, Rb, K, and Na for normal incidence.

TABLE VI. Optical constants of cesium ($T = 195\,°K$).

λ (Å)	$-100(\epsilon_2 \pm \Delta\epsilon_1)$	$\sigma \pm \Delta\sigma$ (10^{12} sec^{-1})	$100(R_0 \pm \Delta R_0)$	$100(n \pm \Delta n)$	$100(k \pm \Delta k)$
6200	133.8+0.7	139+1.5	67.00+0.20	24.2+0.20	118.2+0.3
5780	99.7+0.5	134+1.0	61.80+0.20	25.0+0.15	102.9+0.3
5460	75.0+0.4	134+1.0	55.80+0.20	26.9+0.15	90.6+0.3
5100	48.3+0.3	132.3+0.7	47.20+0.20	29.7+0.10	75.6+0.2
4916	36.1+0.25	130.6+0.7	42.40+0.20	31.5+0.10	67.8+0.2
4600	14.8+0.30	128.0+1.0	31.70+0.20	36.8+0.20	53.3+0.3
4358	−0.5+0.20	126.0+1.0	22.60+0.20	43.2+0.20	42.6+0.3
4060	−18.2+0.20	125.2+0.8	13.10+0.10	53.3+0.10	31.8+0.2
3660	−40.0+0.10	27.6+0.8	5.85+0.04	66.7+0.10	23.3+0.2
3340	−54.0+0.20	135+1.0	3.06+0.03	76.1+0.20	19.7+0.2
3025	−66.6+0.30	149+1.5	1.74+0.03	83.6+0.20	18.0+0.2
2804	−73.7+0.30	163+2.0	1.28+0.03	87.6+0.20	17.3+0.2
2654	−77.0+0.30	168+2.0	1.08+0.03	89.3+0.20	16.7+0.2
2536	−79.8+0.40	168+2.0	0.91+0.03	90.7+0.20	15.7+0.2

Figures 11–13 and Tables X–XIII recapitulate the results, upon which we now briefly comment.

A. Vectorial and spectral selectivity

Three metals (Na, K, Rb) clearly exhibit both vectorial and spectral sensitivity: that is to say,

(i) the true quantum efficiency is different for the same flux power, according to whether the electric vector incident on the surface is $E_\parallel$ or $E_\perp$ (vectorial sensitivity);

(ii) starting from the red end of the spectrum, a sharp maximum appears for Q_λ ($E_\parallel$) for a wavelength λ_m removed from the apparent threshold wavelength by a little more than 1000 Å (spectral selectivity);

(iii) the variations with wavelength of Q_λ ($E_\perp$) show nothing of the kind. This behavior of Q_λ for $E_\parallel$ and $E_\perp$ is more or less classical: It was first detected by Elster and Gëitel as early as 1894 and studied by Pohl and Pringsheim in 1910.

In the region $\lambda \leq \lambda_m$, S_λ and Q_λ for $E_\parallel$ polarization decrease sharply towards a well-marked minimum visible on the curves for potassium and rubidium (Figs. 11 and 12) but which our measuring apparatus could not reach in the case of sodium. This minimum occurs for $\lambda = \lambda_p$, the volume-plasmon wavelength as computed by us from our determinations of the optical constants in the layer. To the best of our knowledge, this experimental fact has not been reported on previously.[18]

Quantum efficiencies for all alkali metals at 195 °K are very low indeed. Table XIV gives relevant value measured at the wavelength corresponding to the maximum sensitivity, λ_m. The maximum efficiency found is for sodium at 3340 Å: 2.3 electrons per 100 absorbed photons. The smallest quantum efficiency throughout is that of cesium, whose highest values in the visible spectrum are of the order of 1.5 electrons emitted for 10 000 photons absorbed. Thus the quantum efficiency decreases in the series with increasing atomic number of the metal considered.

In the spectral region $\lambda < \lambda_P$, the $E_\parallel$ quantum efficiency in the case of potassium and rubidium rises again to reach a second maximum, smaller and more contracted than the first. For reasons already given, the behavior of all four metals in the range $\lambda < 2500$ Å could not be determined.

TABLE VII. Optical constants of rubidium ($T = 195\,°K$).

λ (Å)	$-100(\epsilon_1 \pm \Delta\epsilon_1)$	$\sigma \pm \Delta\sigma(10^{12}$ sec$^{-1})$	$100(R_0 \pm \Delta R_0)$	$100(n \pm \Delta n)$	$100(k \pm \Delta k)$
6200	232+1.4	58.8+2.0	90.90+0.30	8.0+0.2	152.5+0.5
5780	185+1.0	63.0+1.2	88.30+0.30	8.9+0.2	136.1+0.4
5460	152.5+0.8	65.0+1.2	86.10+0.30	9.5+0.2	123.9+0.4
5100	116.3+0.6	66.0+1.0	82.60+0.30	10.4+0.2	108.3+0.3
4916	99.8+0.6	65.5+0.9	80.90+0.30	10.7+0.2	100.5+0.3
4600	71.8+0.4	61.5+0.8	77.50+0.30	11.0+0.1	85.5+0.3
4358	52.0+0.3	58.8+0.7	73.70+0.30	11.7+0.1	73.0+0.2
4060	27.4+0.2	54.3+0.5	65.60+0.30	13.6+0.1	54.0+0.2
3660	−1.3+0.2	53.3+0.6	35.60+0.40	26.8+0.2	24.2+0.3
3340	−21.7+0.1	56.3+0.5	12.80+0.07	48.4+0.1	13.0+0.1
2804	−51.90+0.2	65.5+0.9	2.76+0.04	72.6+0.2	8.4+0.2
2650	−59.8+0.3	71.6+1.5	1.78+0.03	77.7+0.2	8.1+0.2

TABLE VIII. Optical constants of potassium ($T = 195\,°K$).

λ (Å)	$-100(\epsilon_1 \pm \Delta\epsilon_1)$	$\sigma \pm \Delta\sigma (10^{12}\ \text{sec}^{-1})$	$100(R_0 \pm \Delta R_0)$	$100(r \pm \Delta r)$ *	$100(k \pm \Delta k)$
6200	328 + 3	22 + 2.50	97.40 + 0.30	2.3 + 0.30	176 + 1.0
5780	255 + 2	24.60 + 2	96.70 + 0.30	3.0 + 0.20	160 + 0.5
5460	215 + 1.5	28 + 2	95.70 + 0.30	3.5 + 0.25	146.6 + 0.5
4916	151.5 + 0.8	33 + 1.50	93.20 + 0.40	4.4 + 0.20	123.2 + 0.4
4600	117.9 + 0.6	34.70 + 1.50	91.40 + 0.30	4.9 + 0.15	108.7 + 0.3
4358	93.9 + 0.5	32.60 + 1	90.50 + 0.30	4.9 + 0.15	97 + 0.3
4060	64.9 + 0.3	30 + 1	88.50 + 0.30	5.0 + 0.15	80.7 + 0.2
3660	30.4 + 0.2	25.40 + 0.50	84.30 + 0.30	5.6 + 0.10	55.4 + 0.2
3340	5.4 + 0.2	26 + 0.70	65.60 + 0.70	11.2 + 0.30	25.8 + 0.4
3130	−10.1 + 0.15	28.2 + 0.60	25.70 + 0.30	33.0 + 0.20	8.9 + 0.2
2804	−32.0 + 0.1	33.10 + 0.60	7.70 + 0.07	56.8 + 0.10	5.5 + 0.1
2654	−41.3 + 0.15	36.60 + 0.60	4.76 + 0.05	64.5 + 0.10	5.0 + 0.6
2536	−48.0 + 0.3	39.70 + 0.60	3.33 + 0.05	69.4 + 0.15	4.8 + 0.7

B. Comparison with results of other authors

During the contemporary period very few authors seem to have worked on thick layers of alkali metals, *using plane-polarized light*. The only fairly recent measurements of S_λ under conditions similar to ours appear to be those of Brauer, who studied potassium only.[19] The systematic comparison of his results (cf. Fig. 14) with ours shows both similarities and important disagreements. The major disagreement is the fact that in Brauer's work S_λ ($E_\perp$) has clear affinities in its variation with S_λ ($E_\parallel$), and that for the maximum sensitivity the ratio $S_\parallel/S_\perp$ is of the order of 2.7 for Brauer, and 17 in our determinations.

C. The case of cesium

Figure 15 shows that the variations of Q_λ(parallel and perpendicular) with wavelength of the incident flux appear different from the behavior of the same quantities in the case of the three other metals; Q_λ increase with decreasing wavelength in a rather snakelike way, showing no maximum. For $\lambda = \lambda_p$ the curves show nothing of interest and no true minimum. This being noted, let us submit the quantum efficiencies $(Q_\lambda)_\parallel$ and $(Q_\lambda)_\perp$ to a wholly arbitrary treatment: we compute the function ζ_λ of λ, defined by

$$\zeta_\lambda = (Q_\lambda)_\parallel - (Q_\lambda)_\perp \quad .$$

Starting from the threshold wavelength towards decreasing wavelength, ζ_λ features a maximum located at about 4900 Å followed by a well-marked minimum which is again reached for $\lambda \simeq \lambda_p$ (Fig. 15). In the range 2500 Å $< \lambda < \lambda_p$, ζ_λ rises again to a second "plateau": this behavior of ζ_λ is comparable to that of $(Q_\lambda)_\parallel$ for Rb and K, the *relative* importance of the two maximums varying from one metal to another. The likeness increases, and the comparison gets more legitimate if we compute ζ_λ for potassium and rubidium also and show the three functions $\zeta_\lambda = f(\lambda)$ on the same graph (Fig. 16). For the sake of completeness we have added in Fig. 16 the representation of ζ_λ for sodium whose plasma wavelength, and therefore second maximum, if any, lies beyond the short-wave limit of our measurements. In Fig. 15, as well as in

TABLE IX. Optical constants of sodium ($T = 293\,°K$).

λ (Å)	$-100(\epsilon_1 \pm \Delta\epsilon_1)$	$\sigma \pm \Delta\sigma (10^{12}\ \text{sec}^{-1})$	$100(R_0 \pm \Delta R_0)$	$100(n \pm \Delta n)$	$100(k \pm \Delta k)$
6200	715 + 9.0	51 + 6.0	98.2 + 0.3	3.9 + 0.5	273 + 2.0
5780	607 + 7.0	63 + 5.0	97.3 + 0.3	4.9 + 0.4	246 + 1.5
5460	532 + 6.0	71 + 5.0	96.5 + 0.3	5.6 + 0.4	231 + 1.5
4916	413 + 4.0	77 + 4.0	95.3 + 0.3	6.2 + 0.3	203 + 1.0
4600	349 + 3.0	77 + 3.0	94.6 + 0.3	6.3 + 0.3	186 + 0.8
4358	303 + 2.5	74 + 3.0	94.1 + 0.3	6.2 + 0.3	174.1 + 0.7
4060	247 + 2.0	70 + 2.5	93.3 + 0.3	6.0 + 0.2	157.4 + 0.6
3660	185 + 1.0	63 + 2.0	92.4 + 0.3	5.7 + 0.2	136 + 0.4
3340	140 + 0.8	52 + 2.0	92.2 + 0.3	4.9 + 0.15	118.4 + 0.3
3130	110 + 0.6	45 + 1.5	91.9 + 0.3	4.5 + 0.15	105.3 + 0.3
2804	68.7 + 0.5	36 + 1.5	90.8 + 0.4	4.1 + 0.15	83.0 + 0.3
2654	50.7 + 0.5	34 + 2.0	89.5 + 0.5	4.2 + 0.20	71.3 + 0.4
2536	37.3 + 0.4	32 + 2.0	87.9 + 0.5	4.4 + 0.20	61.3 + 0.4

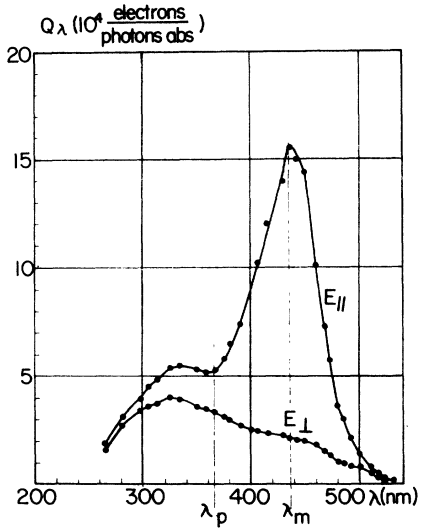

FIG. 11. "True" quantum efficiency of rubidium, $\varphi = 45°$.

the figures representing $(Q_\lambda)_{II}$, we note that the *relative* importance of the second (short-wave) maximum is large for cesium, much smaller but well defined for rubidium, and smaller still in the case of potassium. We note also in Fig. 16 that the shape of all four curves in the region of the first maximum of ζ_λ is very much alike that of resonance curves.

True quantum efficiencies are almost never mentioned in the literature on photoemission. Figure 17, which sums up our results (for E_{II}) in terms of emissivities, will enable the reader easy comparison with previous publications.

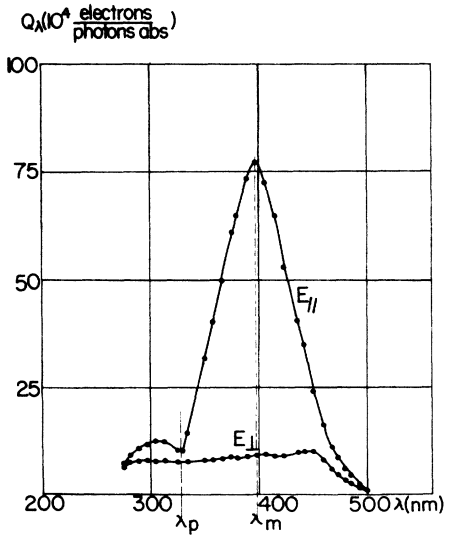

FIG. 12. "True" quantum efficiency of potassium, $\varphi = 45°$.

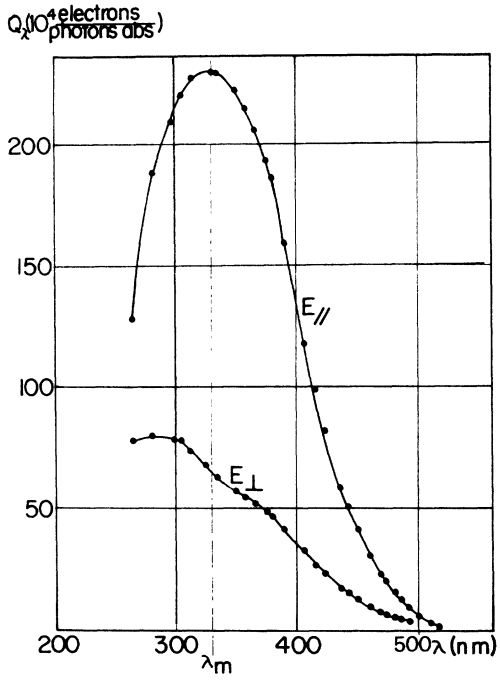

FIG. 13. "True" quantum efficiency of sodium, $\varphi = 45°$.

V. OPTICAL AND PHOTOELECTRICAL PROPERTIES OF THICK LAYERS IMMEDIATELY AFTER THEIR PREPARATION AT 77 °K

In Sec. II we have described the procedure followed for the deposition of the metal layers. The reader will remember that the condensation of the metal vapor onto the target is carried on at temperature 77 °K. The finished layers are kept at this temperature during measurement of their optical and photoelectrical properties. In this section we shall compare the properties of the layers before heating, to their properties after heating at 195 °K and 293 °K, which have just been described in Sec. III.

A. Reproducibility

The reproducibility of the various surface properties from layer to layer is far from being as good at deposition as it becomes after heating at 195 °K. The optical properties may shift from one layer to another, the range of variation being ± 5%. The photoemission range of variation is larger still (± 12% and even 15%). This suggests that a random parameter, active during the deposition procedure, disappears on heating the layers at 195 or 293 °K, as was assumed already in Sec. IV.

TABLE X. Emissivity S_λ and "true" quantum efficiency Q_λ of cesium, $\varphi = 45°$, $T = 195\,°K$.

λ (Å)	S_λ (μA/W) $E_\parallel$	S_λ (μA/W) $E_\perp$	$10^4 Q_\lambda$ (electrons/abs. photon) $E_\parallel$	$10^4 Q_\lambda$ (electrons/abs. photon) $E_\perp$
5550	3.0	1.5	0.14	0.124
5460	4.5	2.1	0.21	0.17
5400	7.0	2.8	0.32	0.22
5300	10.2	3.7	0.47	0.29
5230	12.5	4.3	0.57	0.33
5100	15.7	5.5	0.70	0.41
5000	17.5	7.0	0.76	0.51
4850	22.0	8.3	0.94	0.58
4730	24.5	10.6	1.02	0.71
4600	27.0	12.4	1.10	0.80
4500	29.0	14.9	1.16	0.94
4360	32.0	17.5	1.24	1.05
4230	36.5	20.3	1.39	1.16
4060	43.0	24.7	1.61	1.32
3900	52.0	29.6	1.91	1.50
3800	58.0	32.1	2.12	1.57
3660	63.5	35.5	2.32	1.62
3500	69.0	38.5	2.56	1.73
3340	73.5	41.0	2.79	1.80
2967	68.0	39.8	2.85	1.9
2804	65.0	42.8	2.90	2.0
2650	63.0	41.0	2.96	2.02

TABLE XII. Emissivity S_λ and "true" quantum efficiency Q_λ of potassium, $\varphi = 45°$, $T = 195\,°K$.

λ (Å)	S_λ (μA/W) $E_\parallel$	S_λ (μA/W) $E_\perp$	$10^4 Q_\lambda$ (electrons/abs. photon) $E_\parallel$	$10^4 Q_\lambda$ (electrons/abs. photon) $E_\perp$
5000	2.8	1.6	0.9	1.02
4916	7.2	2,64	2.2	1.6
4850	15.1	4.25	4.5	2.5
4730	30.5	8.40	8.7	4.7
4600	60.0	14.90	16.4	7.9
4500	91.5	19.70	24.2	10.2
4360	137.0	19.20	35.7	9.8
4230	207.0	18.20	53.0	9.1
4150	257.0	18.40	65.0	9.0
3980	303.0	18.60	77.5	9.1
3900	290.0	18.40	73.6	9.0
3800	255.0	17.90	65.0	8.7
3660	206.0	18.00	50.0	8.5
3500	141.0	18.8	32.0	8.1
3340	73.0	20.4	14.5	7.7
3250	58.0	22.6	10.5	7.6
3130	77.0	27.0	12.3	7.9
2970	92.0	34.7	11.9	8.1
2895	93.5	38.0	11.0	7.8
2804	94.0	44.0	9.3	7.7
2650	83.5	45.0	6.3	5.4

B. Optical properties at 77 °K

For the three metals Na, K, Rb, the behavior is the same:

(i) The variations of the real part of the dielectric constant ϵ_1 with λ^2 does *not* follow the Cohen relation [Eq. (1)] as it did at 195 °K, and the departure from this linear law is noticeable for Rb, important in the case of K, and enormous in the

TABLE XI. Emissivity S_λ and "true" quantum efficiency Q_λ of rubidium, $\varphi = 45°$, $T = 195\,°K$.

λ (Å)	S_λ (μA/W) $E_\parallel$	S_λ (μA/W) $E_\perp$	$10^4 Q_\lambda$ (electrons/abs. photon) $E_\parallel$	$10^4 Q_\lambda$ (electrons/abs. photon) $E_\perp$
5230	1.75	1.0	0.23	0.10
5170	3.4	1.43	0.42	0.34
5100	6.2	1.93	0.74	0.43
5000	11.7	3.22	1.40	0.73
4850	25.0	4.3	3.0	0.93
4730	51.0	6.2	5.7	1.30
4680	65.0	7.2	7.3	1.50
4600	92.0	8.6	10.1	1.80
4500	133.0	9.7	14.4	2.00
4360	147.0	10.8	15.6	2.12
4230	134.0	12.0	14.0	2.30
4060	102.0	13.5	10.2	2.50
3900	79.0	15.9	7.4	2.70
3800	72.0	18.9	6.5	2.00
3660	64.0	22.6	5.3	3.30
3500	71.0	28.0	5.3	3.60
3340	82.0	36.0	5.5	3.90
3130	86.0	43.0	4.8	3.7
2967	79.0	48.0	3.9	3.4
2804	65.0	46.0	3.1	2.7

TABLE XIII. Emissivity S_λ and "true" quantum efficiency Q_λ of sodium, $\varphi = 45°$, $T = 293\,°K$.

λ (Å)	S_λ (μA/W) $E_\parallel$	S_λ (μA/W) $E_\perp$	$10^4 Q_\lambda$ (electrons/abs. photon) $E_\parallel$	$10^4 Q_\lambda$ (electrons/abs. photon) $E_\perp$
5100	7.35	2.25	3.00	1.36
5000	14.40	3.70	5.90	3.00
4916	23.50	4.80	9.40	3.80
4850	31.80	6.10	12.50	4.70
4730	52.50	9.05	20.20	6.80
4600	82.20	13.80	31.00	10.10
4500	111.00	17.50	41.30	13.00
4360	162.00	24.00	59.00	17.50
4230	225.00	32.90	82.00	23.50
4060	328.00	46.20	118.00	33.00
3900	445.00	60.00	159.00	42.00
3800	520.00	67.10	186.00	47.00
3660	578.00	73.30	206.00	52.00
3500	590.00	78.40	222.00	57.00
3340	580.00	82.20	230.00	63.00
3250	558.00	85.70	227.00	68.00
3130	545.00	90.70	228.00	74.00
3050	511.00	94.50	220.00	78.00
2970	480.00	91.20	209.00	78.00
2804	416.00	90.80	188.00	80.00

TABLE XIV. Maximal quantum efficiency for alkali metals (photoemission).

Metal	Na	K	Rb	Cs
λ_m (Å)	3340	3880	4360	4900
$S_{\parallel}\left(\frac{\mu A}{W}\right)$	590	300	146	19
$S_{\parallel}\left(\frac{\text{electrons}}{\text{abs. photon}}\right)$	23×10^{-3}	77×10^{-4}	16×10^{-4}	8×10^{-5}
$\frac{Q_{\parallel}}{Q_{\lambda}}(\lambda_m)$	3.6	8.5	8.0	1.5

case of Na (Fig. 18).

(ii) The behavior of the "optical conductivity" or absorption coefficient $\sigma=\epsilon_2\epsilon_0\omega$ is profoundly altered, as Fig. 19 will show. In the case of rubidium and potassium, the variation of σ with the wavelength is very similar to the curves delineated at 195 °K in the range $\lambda<\lambda_p$. On the contrary, in the range $\lambda>\lambda_p$, the optical conductivities at 77 °K are remarkable for the sharp and important maximum which they feature and which occur at a wavelength a little greater than the surface-plasmon wavelength λ_s, as computed from the experimental data obtained at 195 °K. Figure 19 shows the behavior of sodium; we have not followed the variations of σ till the *volume*-plasmon wavelength, which is located somewhere in the neighborhood of 2210 Å; it is quite possible that the general shape of σ for sodium is really similar to that of the two other metals investigated.

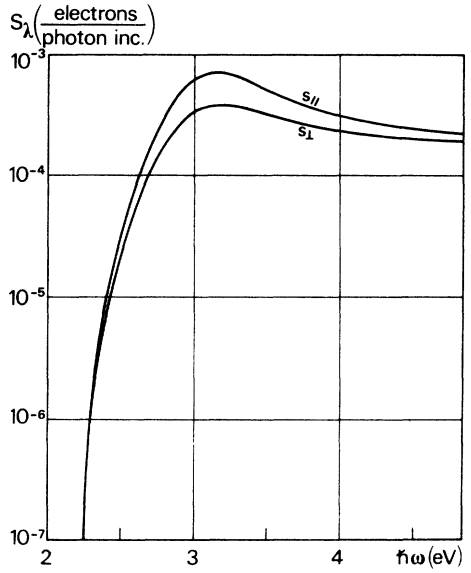

FIG. 14. Emissivity of potassium, in electron per incident photons: Brauer's results for $\varphi=45°$ and $T\simeq293$ °K.

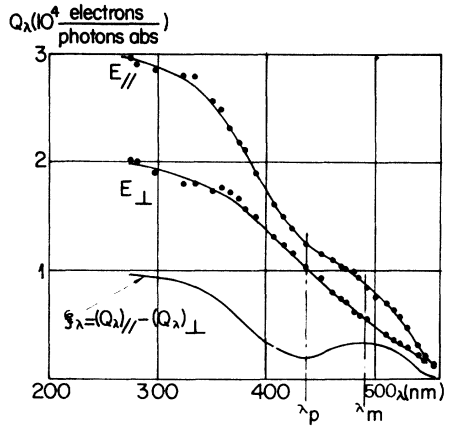

FIG. 15. "True" quantum efficiency of cesium, $\varphi=45°$.

(iii) The computation of the normal reflectivity R_0 of the 77 °K surfaces gives very remarkable results: for Rb, K, Na, in the short-wavelength range $\lambda_x>\lambda_p>\lambda$, starting from a wavelength λ_x, which has no particular association, the reflectivity at 77 °K is practically the same as at 195 °K (Fig. 20). On the contrary, in the range $\lambda_x>\lambda$ instead of finding, as at 195 °K, a monotonic increase of R_0 with increasing wavelength, the 77 °K R_0 curve exhibits an anomaly corresponding to a decrease of reflecting power extending roughly over the range 4200–6700 Å for rubidium, 3600–6200 Å for potassium, and over the whole range of our measurements for sodium. The largest deviation

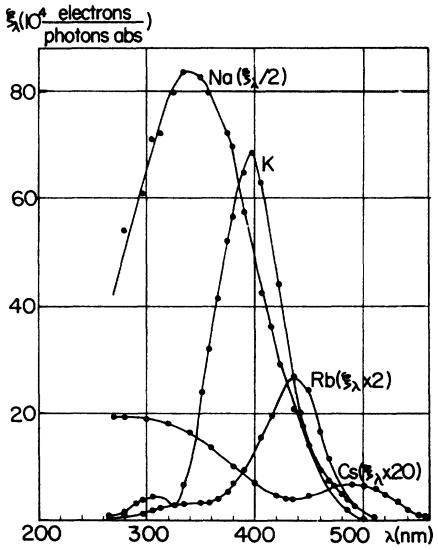

FIG. 16. Curves representing $\xi\lambda=Q(E_{\parallel})-Q(E_{\perp})$, for Cs, Rb, K, and Na; incidence angle 45°.

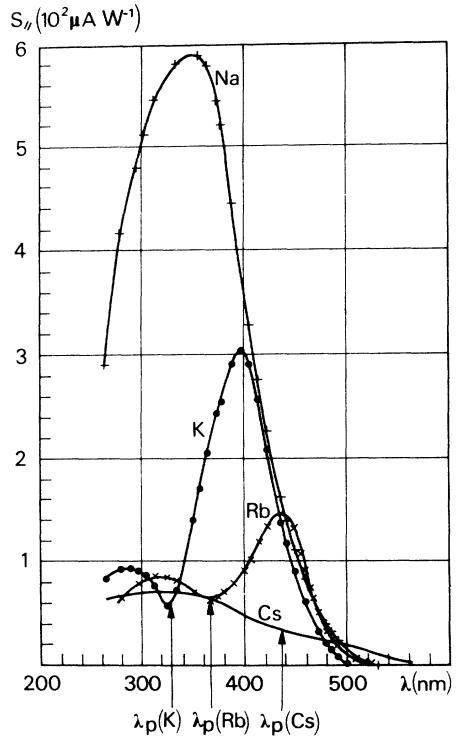

FIG. 17. Photoelectric emissivities of Cs, Rb, K, and Na for polarized light ($E_{//}$), $\varphi = 45°$.

of R_0(77 °K) compared with R_0(195 °K) in this anomalous domain is given in Table XV.

One may point out that the general shape of these $R_0(77\ °K) = f(\lambda)$ curves is similar to that of the R_0 curves for silver[20] and aluminium[21,22] artificially "roughened," in the range of wavelength containing λ_s.

One should recall that the computation of R_0 is based in all cases on ellipsometer measurements; the divergence of the light beam used in the ellipsometer being of the order of a few minutes of an arc, we are therefore unable to indicate which part, if any, of the anomalous decrease of R_0 (77 °K) in the long-wavelength range is caused by absorption and which part by diffusion.

C. Photoemission and quantum efficiency

The three metals Rb, K, and Na exhibit the same behavior, which is summed up by Fig. 21. At 195 °K, the stabilized layers exhibit both *spectral* and *vectorial* sensitivity, the case of $E_{//}$ polarization showing alone a sharp maximum of quantum efficiency near the threshold.

As seen from Fig. 21, the same layers, studied at 77 °K immediately after deposition show that the curves $Q_{//}$ and $Q_{\perp}$ are now very similar. In fact, one may speak of affinity between the two, since multiplication of the ordinates of one of them by a correctly chosen numerical factor will bring them to a fair coincidence: the simplest explanation of this behavior is that the surface of a layer prepared and kept at 77 °K has nothing to do with a plane or a mosaic of large planar regions with a preferred orientation but, on the contrary, that they are made of a multitude of microcrystals with their facets oriented in a more-or-less random manner according to whether the mobility of the metallic atoms condensing on the cooled target is zero or only small. Such a hypothesis would also explain why the reproducibility of the properties from our layer to another is not as good as it is for layers "stabilized" at 195 or 293 °K (see above).

However, on the Q_λ(77 °K) curves one can distinguish not only a maximum for nearly the same wavelength as that of the 195 °K maximum, but also the minimum for λ_p (the volume-plasmon wavelength) already noted in the stabilized layers. These two characteristics, therefore, appear to be properties of the element itself, and only slightly (or not at all) dependent on the state of crystallization of the layers or their surface geometry.

D. The case of cesium

The layers of cesium prepared and measured at 77 °K without any prior reheating have optical and photoelectrical properties only slightly different from what they become at 195 °K. As seen in Fig. 18, the Cohen relation is almost verified; the very important and sharp maximum of the op-

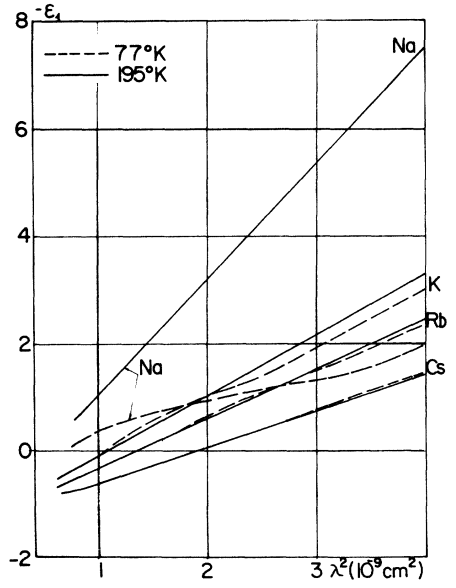

FIG. 18. ϵ_1 vs λ^2 for Cs, Rb, K, and Na, at 77 °K (-----) and at 195 °K (———) (293 °K for Na).

tical conductivity present at 77 °K for rubidium potassium, and sodium, is here nonexistent [Fig. 19(a)]; again, the reflecting power R_0 is practically the same at both temperature, [Fig. 20(a)]. Finally, the Q_λ curves, though showing a little more spectral selectivity than is the case for 195 °K, remain very similar to what they are after heating. All this suggests, of course, that the mobility of cesium atoms falling on glass or on cesium kept at 77 °K is far from negligible and that even at this low temperature, extensive rearrangement has already taken place. The behavior of $\xi = (Q_\lambda)_\parallel - (Q_\lambda)_\perp$ at 77 °K is very similar to what it is at 195 °K.

E. Comparison with results of other authors

The modern literature is very poor on data concerning the bulk properties of alkali metals, or thick layers of these, especially with polarized light. The recent determinations of Smith[1] and Van Oirschot[5] have been made with unpolarized light. The well-known work of Ives and Briggs[3] has been done entirely with *thin* layers. The only measurements that were made under more-or-less

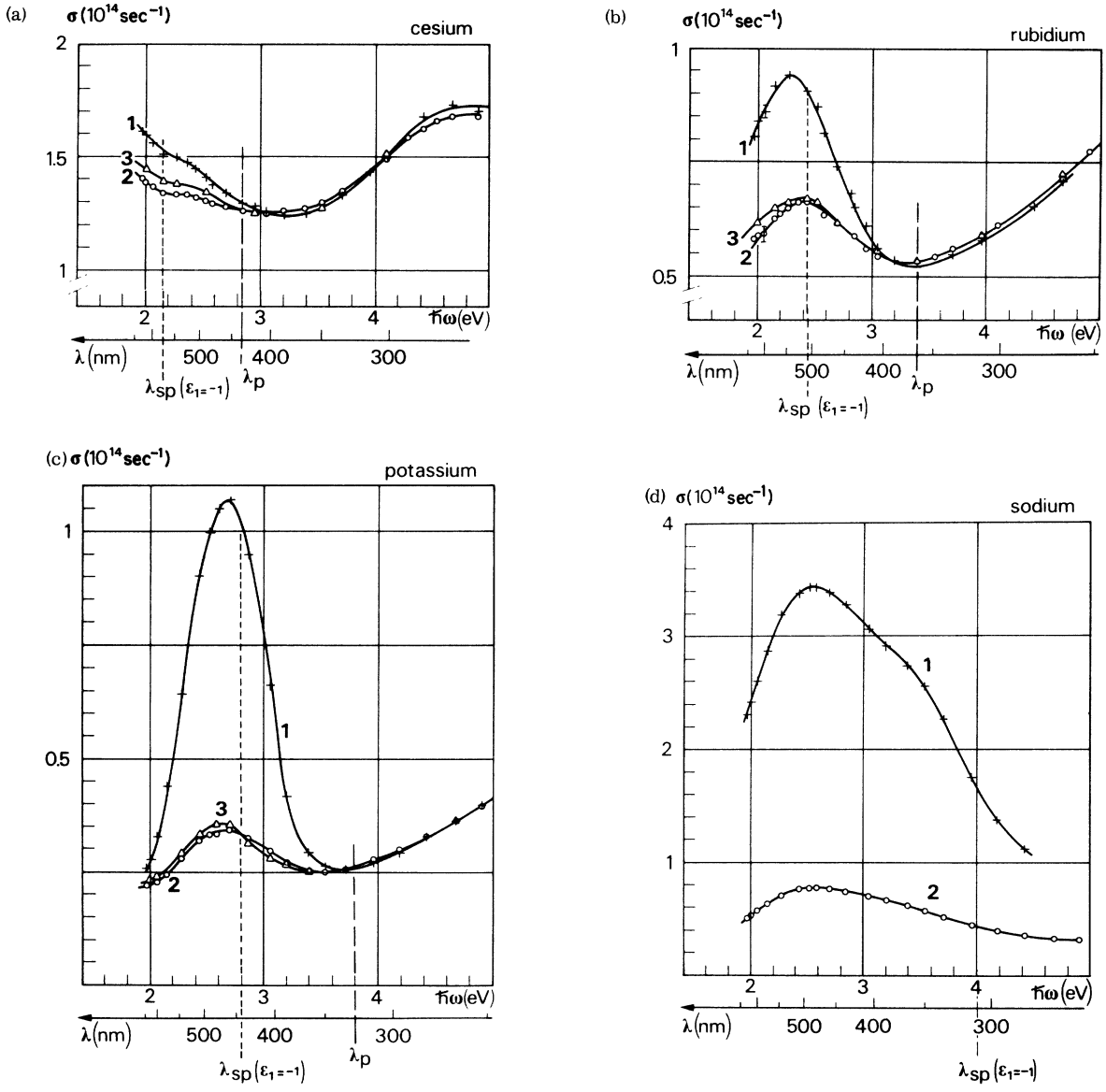

FIG. 19. (a) Optical conductivity of cesium at 77 °K (1), 195 °K (2), 77 °K (3) (after recooling). (b) Optical conductivity of rubidium at 77 °K (1), 195 °K (2), 77 °K (3) (after recooling). (c) Optical conductivity of potassium at 77 °K (1), 195 °K (2), 77 °K (3) (after recooling). (d) Optical conductivity of sodium at 77 °K (1) and 293 °K (2).

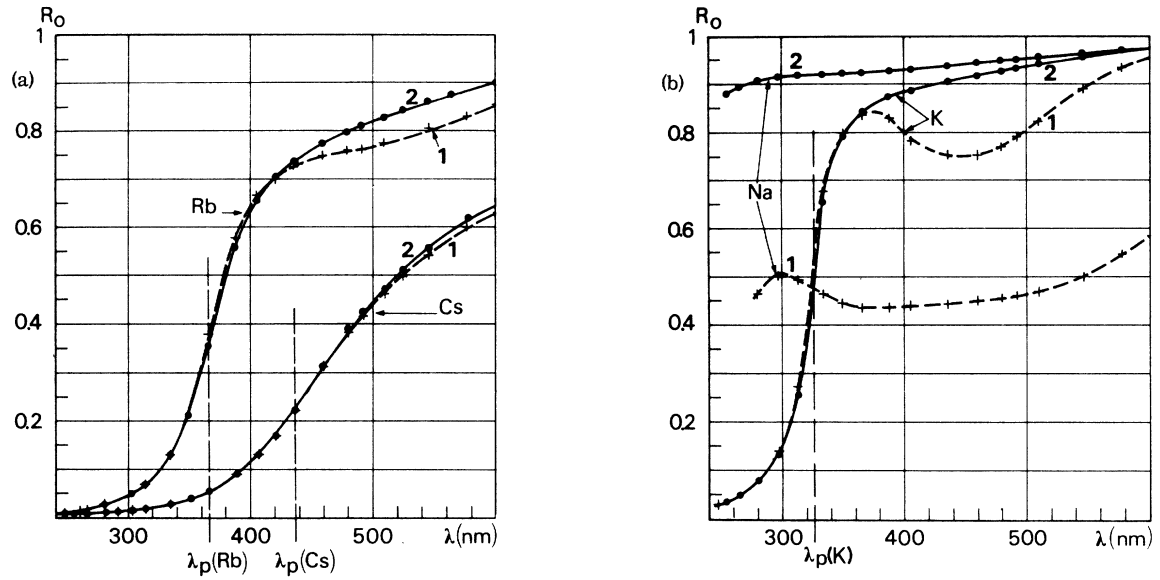

FIG. 20. (a) Reflectivity of Cs and Rb at normal incidence: 77 °K (1), 195 °K (2). (b) Reflectivity of [77 °K (1) and 195 °K (2)] and Na [77 °K (1) and 293 °K (2)], for normal incidence.

similar conditions as ours have been performed by Mayer *et al.*[2]

Figure 22 shows Mayer's results obtained at 77 °K. He finds two maxima, one for $(S_\lambda)_{\parallel}$ at 3660 Å and one for $(S_\lambda)_\perp$ at 4280 Å; this last value is close to the single maximum which we find *both* for $E_{\parallel}$ and for $E_\perp$.

VI. BEHAVIOR OF LAYERS DURING DEPOSITION

As a control, and to follow the variations of the properties of the surface of each layer during deposition, ellipsometric and photoelectric measurements were made during the whole of the deposition period. Deposition was suppressed only when the optical and photoelectrical properties thus followed has remained constant during a sufficient interval of time.

Let us accept that, during the whole time of processing, the evaporation speed was small enough to ensure a molecular flow regime. If P_s is the vapor pressure at a temperature T, and on condition that the reflection coefficient for alkali-metal atoms falling on a target at 77 °K is negligible, the speed of deposition at the time t may be written

$$\frac{dm}{dt} = \left(\frac{M}{2\pi R}\right)^{1/2} T^{-1/2} P_s \quad .$$

In our experiments, T increased slowly and regularly with time t, so that one could write that, within an acceptable margin of error,

TABLE XV. Largest difference of reflectivities at 195 and 77 °K.

Metals	λ (Å)	R_0(77 °K) (minimum)	R_0(77 °K)/R_0(195 °K)
Rb	5200	0.78	0.93
K	4600	0.75	0.78
Na	3700	0.44	0.48

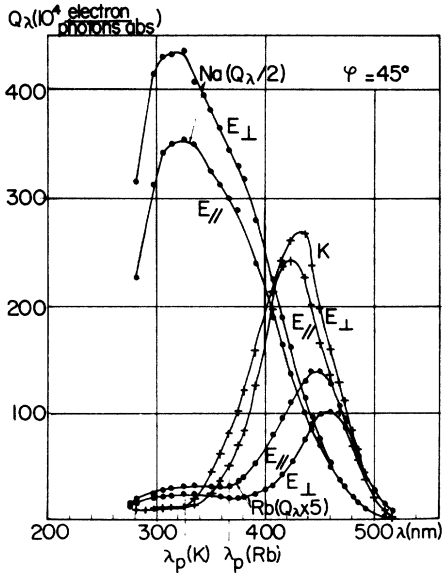

FIG. 21. "True" quantum efficiency of Rb, K, and Na, at 77 °K (before any heating), for an incidence angle of 45°.

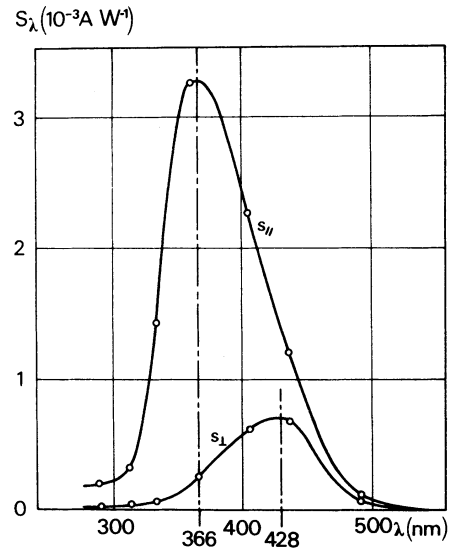

FIG. 22. Photoelectric emissivity of potassium at 77 77 °K: Mayer's results.

$$T = T_0 + at \quad .$$

The mass deposited on unit surface of the target during the interval of time marked by the temperature T_0 and T_x is therefore given by

$$m = A\left(\frac{M}{2\pi R}\right)^{1/2}\frac{1}{a}\int_{T_0}^{T_x}\frac{P_s}{\sqrt{T}}\,dT \quad ,$$

in which A is a number dependent on the geometry and dimensions of the setup. The equation

$$\ln P_s = \alpha - \beta/T$$

represents the variations of p_s with sufficient accuracy; α and β have been measured by prior experimenters.[23] On condition that the specific mass of the metal condensed on the layer is identical with the specific mass of the bulk metal (we have to assume it is), we can determine from the preceding equations the thickness obtained after a given interval of time.

The optical property measured during deposition was the ratio of the two coefficients of optical reflection, $\tan\psi = |r_{\parallel}/r_{\perp}|$ whose value is given by a single ellipsometric determination. The emission $(S_\lambda)_{\parallel}$ was continuously recorded.

Figure 23 is an example of the results; this example depicts the deposition of potassium on the target, while measuring $\tan\psi$ and $S_{\parallel}$ both with 3130-Å plane-polarized light (a wavelength close to the domain of maximum transparency of the bulk metal). All four metals gave similar results: both $\tan\psi$ and $S_{\parallel}$ show pronounced maxima for different thicknesses of the layer, to fall again sharply through a short range of increasing thickness. Finally, the layer achieves a thickness such that and $(S_\lambda)_{\parallel}$ do not change with further increase in thickness. In the example of Fig. 23, this thickness is seen to be about 5000 Å; in this example, deposition was continued till the thickness increased up about 20 000 Å. The same remarks apply to the growth of Rb layers. In the case of cesium, we have found a difference between "photoelectric thickness" (3000 Å) and "optical thickness" (7000 Å) with $\lambda = 3660$ Å. Sodium was not investigated. These results are, again, at variance with those of the Mayer group.[2]

VII. ALKALI METALS AND THE FOWLER ANALYSIS OF RESULTS

We do not reproduce here the calculation of Fowler, which can be considered as classical. Denoting true threshold coefficients at 0 °K by the subscript zero (ω_0, λ_0, w_0), the Fowler equation may be written in terms of the photoelectric current density

$$J = AT^2 f\left(\frac{\hbar\omega - \hbar\omega_0}{kT}\right) \quad ,$$

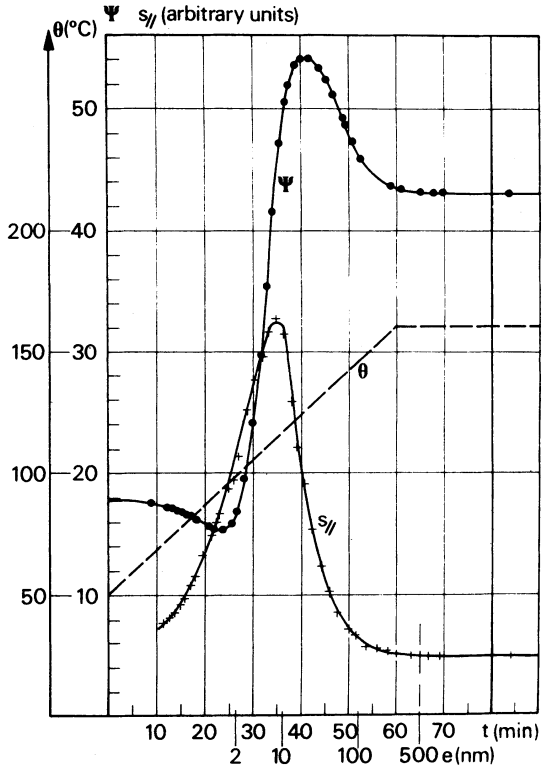

FIG. 23. Values of $S_{\parallel}$ and $\psi = \arctan(r_{\parallel}/r_{\perp})$ as a function of thickness (and deposition time) of a potassium film. Substrate glass, condensation temperature 77 °K. Excitation, monochromatic radiation $A = 3130$ Å; $E_{\parallel}$ polarized.

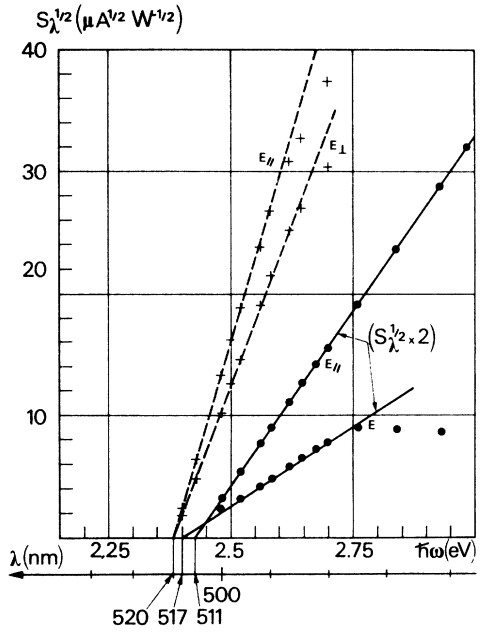

FIG. 24. Square root of photoelectric yield as a function of photon energy for potassium, at 77 °K ($E_{\parallel}$ and $E_\perp$) and at 195 °K ($E_{\parallel}$ and $E_\perp$).

where f is the well-known Fowler function. Provided that $\hbar\omega - \hbar\omega_0 \gg kT$, one can simplify this expression and write

$$J^{1/2} \simeq \left(\frac{2\pi\Gamma em}{\hbar^3}\right)^{1/2} (\hbar\omega - \hbar\omega_0) \quad .$$

This means that, provided we do not get too close to the 0 °K threshold nor extend our plotting so far that Γ, the photon-electron probability interaction ceases to be constant, the simplified Fowler equation

$$J^{1/2} = f(\hbar\omega)$$

will represent a straight line.

We have therefore plotted against $\hbar\omega$ the values of $(S_\lambda)_{\parallel}^{1/2}$ and $(S_\lambda)_\perp^{1/2}$ for the four metals at 77 °K, $(S_\lambda)_{\parallel}^{1/2}$ and $(S_\lambda)_\perp^{1/2}$ for K, Rb, and Cs at 195 °K, and $(S_\lambda)_{\parallel}^{1/2}$ and $(S_\lambda)_\perp^{1/2}$ for Na at 293 °K.

Actually one gets a rectilinear segment in all cases, extending from close to the true threshold: $\hbar\omega - \hbar\omega_0 > 0.025$ eV at 77 °K, 0.063 eV at 195 °K, 0.095 eV at 293 °K, through a spectral interval of several hundred angstrom (up to 1000 Å for sodium). From these rectilinear segments, the threshold at 0 °K was obtained by linear extrapolation. Figure 24 gives the results for potassium, five distinct layers of which have been measured the results in each case being put through the Fowler process. The three other metals behave in the same way which may be summed up as follows (see Table XVI):

(i) The work function W_0 for an alkali metal is not the same before and after reheating the layer;

(ii) at 77 °K, the curves $(S_\lambda)_{\parallel}$ and $(S_\lambda)_\perp$ (we have noted their affinity) yield the same value of the work function;

(iii) on the contrary, the layers stabilized by reheating at 195 °K (or 293 °K) show two different values of the work function W_0 according to whether the incident light is polarized parallel or perpendicular. The work function corresponding to $(S_\lambda)_{\parallel}$ is always larger than the other by several hundredths of an electron volt. This small difference is very reproducible and cannot be assigned, to the best of our knowledge, to systematic errors in measurement.

VIII. CONCLUSIONS

In concluding we call the reader's attention to the following main results:

(i) The "true" quantum efficiency of the alkali metals never exceeds 2% for sodium, 0.8% for potassium, 0.16% for rubidium, or 0.03% for cesium. Thus photoemission in these metals appears as a second-order phenomenon when compared with the whole photon absorption.

(ii) A *nonvectorial* spectral selectivity is observed on layers prepared and kept at 77 °K. After slow heating to 195 °K (293 °K for sodium), *vectorial selectivity* sets in: the selective spectral sensitivity is observable only when the electric vector in the incident wave is parallel to the plane of incidence ($E_{\parallel}$). In the opposite case ($E_\perp$) a sensitivity is observed which does *not* feature spectral selectivity, but a monotonic variation with λ. Further cooling does not modify the properties of such layers: the transformation induced by the heating is irreversible and it is accompanied by the collapse of the $S_\perp$ and $S_{\parallel}$ values, a collapse that is larger the smaller the atomic number of the metal concerned. The probability is large that this irreversible transformation is induced by a modification of the layer structure and of its surface geometry (e.g., at 77 °K a "rough" structure which disappear when the layer is heated).

(iii) When the Fowler "extrapolation" is performed on the $(S_\lambda)_{\parallel}$ and $(S_\lambda)_\perp$ curves, in the case of

TABLE XVI. Work function of alkali metals at 77 and 195 °K.

Metal	W_0(77 °K) in eV $E_{\parallel}$ or $E_\perp$	W_0(195 °K) in eV $E_{\parallel}$	$E_\perp$
Cs	2.09 + 0.01	2.11 + 0.01	2.05 + 0.01
Rb	2.31 + 0.01	2.31 + 0.01	2.20 + 0.01
K	2.38 + 0.01	2.43 + 0.01	2.40 + 0.01
Na	2.37 + 0.01	2.34 + 0.01	2.27 + 0.01

layers prepared and kept at 77 °K, both curves extrapolate to a *single* well-defined work function at 0 °K, W_0 (reproducibility better or equal to 0.01 eV); in the case of layers heated at 195 °K or 293 °K, two different work functions result, one, $W_{0\parallel}$, corresponding to the extrapolation of $(S_\lambda)_\parallel^{1/2}$, the other, $W_{0\perp}$, being given by the extrapolation of $S_\perp^{1/2}$. $W_{0\parallel}$ and $W_{0\perp}$, though differing *only by a few hundredths of electron volt*, are as reproducible as W_0 determined at 77 °K.

(iv) In the case of K and Rb, the emission $(S_\lambda)_\parallel$ and true quantum efficiency $(Q_\lambda)_\parallel$ curves both show a well-defined minimum when the wavelength of the incident radiation is equal to the volume-plasmon wavelength λ_p. $(S_\lambda)_\perp$ and $(Q_\lambda)_\perp$ show nothing of the kind. In the case of cesium the curves $(S_\lambda)_\parallel$ and $(Q_\lambda)_\parallel$ only show an inflection when $\lambda = \lambda_p$. Sodium could not be studied in that aspect, λ_p being too far in the uv ($\lambda_p \simeq 2200$ Å) for this metal.

(v) The curves obtained for K, Rb, and Cs by plotting the variations of the reflecting power at normal incidence R_0 show a point of inflection at the volume-plasmon wavelength λ_p. At this point, the slope of each $R_0 = f(\lambda)$ curve is maximum, and the value of this becomes larger as the atomic number of the metals decrease.

---

[1]N. V. Smith and W. E. Spicer, Phys. Rev. 188, 593 (1969). N. V. Smith, Phys. Rev. 183, 634 (1969).

[2]H. Mayer and H. Thomas, Z. Phys. 147, 419 (1957); H. Thomas, Z. Phys. 147, 395 (1967).

[3]H. E. Ives *et al.*, Phys. Rev. 38, 1209 (1931); Phys. Rev. 39, 1447 (1932); Phys. Rev. 40, 802 (1932); J. Opt. Soc. Am. 23, 73 (1933); J. Opt. Soc. Am. 26, 238 (1936); J. Opt. Soc. Am. 27, 181 (1937).

[4]In the case of sodium, the following crystalline structures have been identified: body-centered cubic (4.24 Å at 77 °K); face-centered cubic (5.34 Å at 77 °K); hexagonal ($a = 3.767$ Å; $c = 6.154$ Å at 5 °K). For more informations, see Aruja and Perlitz, Z. Kristallogr. 100, 195 (1938); Barrett, Am. Mineral. 33, 749 (1948); J. Inst. Met. 84, 43 (1955); Acta Crystallogr. 9, 671, (1956).

[5]T. G. J. Van Oirschot, Ph. D. thesis (Leiden University, Netherlands, 1970) (unpublished).

[6]J. C. Richard (private communication). G.-A. Boutry and H. Dormont, Philips Tech. Rev. 30, 225 (1969).

[7]See, for instance, A. C. Hardy, P. J. Fopiano, and M. P. Trageser, U. S. Patent No. 2 974 561, (1961); M. Billardon, thèse 1960 (Masson & Co., Paris, 1962) (unpublished); S. S. Williamson, J. M. Weingart, and R. D. Andrews, J. Opt. Soc. Am. 54, 337 (1964); A. B. Winterbottom, Natl. Bur. Stand. Misc. Publ. No. 256 (U. S. GPO, Washington, D. C., 1964), pp. 97–112.

[8]J. Monin, J. Houdard, and G.-A. Boutry, C. R. Acad. Sci. (Paris) 267, 1078 (1968); C. R. Acad. Sci. (Paris) 270, 200 (1970).

[9]J. Monin, thèse de Doctorat (Université Paris VI, 1972) (unpublished), pp. 59–60.

[10]M. H. Cohen, Philos. Mag. 3, 762 (1958).

[11]U. S. Whang, E. T. Arakawa, and T. A. Calcott, J. Opt. Soc. Am. 61, 740 (1971).

[12]N. V. Smith, Phys. Rev. B 2, 2840 (1970).

[13]H. Mayer and B. Hietel, in *Optical Properties and Electronic Structure of Metals and Alloys*, edited by F. Abelès (North-Holland, Amsterdam, 1966), p. 47.

[14]A. H. Wilson, *The Theory of Metals* (Cambridge U. P., New York, 1936), p. 133.

[15]P. N. Butcher, Proc. Phys. Soc. A 64, 50 (1951).

[16]N. Ashcroft, Phys. Rev. 140, A935 (1965).

[17]N. V. Smith, Phys. Rev. B 183, 634 (1969).

[18]It has been predicted by J. G. Endriz in Phys. Rev. B 7, 3464 (1973), which was published after this manuscript had been submitted for publication. The comparison of Fig. 9 of the Endriz paper and Fig. 16 of this paper will show a remarkable agreement between theory and experiment.

[19]M. Brauer, Phys. Status Solidi, 14, 413 (1966).

[20]P. Dobberstein, A. Hampe, and G. Sauerbrey, Phys. Lett. 27A, 256 (1968).

[21]J. G. Endriz and W. E. Spicer, Phys. Rev. B 4, 4144 (1971); Phys. Rev. B 4, 4159 (1971).

[22]A. Daudé, A. Savary, and S. Robin, J. Opt. Soc. Am. 62, 1 (1972).

[23]S. Dushmann, *Vacuum Technique* (Wiley, New York, 1949).

[24]C. Kunz, Z. Phys. 196, 311 (1966).

[25]U. S. Whang, E. T. Arakawa, and T. A. Calcott, Phys. Rev. B 5, 2118 (1972).

[26]J. Brambring, Z. Phys. 200, 186 (1967).

[27]J. C. Sutherland and E. T. Arakawa, J. Opt. Soc. Am. 58, 1080 (1968).

[28]R. E. Palmer and S. E. Schnatterly, Phys. Rev. B 4, 2329 (1971).